

Anion Titration Studies of Tetraamide Compounds as a Potential Chromate Separation Materials

Maisara Abdul Kadir^{a,*}, Fazira Ilyana Abdul Razak^b, Nur Shuhaila Haryani Haris^a

^a Faculty of Science and Marine Environment, Universiti Malaysia Terengganu, 21030 Kuala Nerus, Terengganu

^b Department of Chemistry, Faculty of Science, Universiti Teknologi Malaysia, 81310, UTM Johor Bahru, Johor, Malaysia

Article history

Received

20 August 2023

Revised

26 September 2023

Accepted

15 October 2023

Published online

25 November 2023

*Corresponding author
maisara@umt.edu.my

Abstract

This study describes the synthesis and characterization of two tetraamide compounds namely, 1,2-bis[*N,N'*-6-(4-pyridylmethylamido)pyridyl-2-carboxyamido]ethane (L1) and 1,2-bis[*N,N'*-6-(4-pyridylmethylamido)pyridyl-2-carboxyamido]propane (L2) which were prepared by reacting *N*-6-[(4-pyridylmethylamino)carbonyl]-pyridine-2-carboxylic acid methyl ester with ethane-1,2-diamine and propane-1,3-diamine, respectively. These types of compounds are commonly studied for anion separation materials due to their pre-organized structure that is readily intended to capture anion via hydrogen bonding. Characterization of L1 and L2 was conducted by Fourier Transform Infrared spectroscopy (FTIR), ¹H and ¹³C Nuclear Magnetic Resonance (NMR). The structure conformation was supported by theoretical studies which were conducted through DFT analysis. Evaluation of the potential of these compounds to interact with chromate anions was investigated using the UV-Vis titration technique. The results showed that L1 has a good affinity towards chromate anions compared to L2. This result concluded that the utilization of smaller spacer units such as ethyl contributed to the ease of binding of a molecular host to chromate anions through NH amide binding pockets, compared to the use of a lengthier spacer.

Keywords Amide, anion, chromate, anion titration, anion binding

© 2023 Penerbit UTM Press. All rights reserved.

1.0 INTRODUCTION

Anionic compounds show a significant contribution to our daily lives, particularly in the fields of agriculture and industrial activities. Anions such as nitrates and phosphates are frequently found in agricultural fertilizers that reach into lakes, and streams from many sources such as septic systems, animal food, sanitary landfills, garbage dumps, domestic sewage and industrial wastewaters [1-3]. It is also known to all that excess concentration of nitrate and phosphate allows huge growth of water plants that possibly leads to eutrophication which has threatened innumerable aquatic life [4].

Instead of these two anions that particularly play major contributions in our lives, few anions need serious attention, such as chromate anions. Chromate anion is commonly used in textile industries, as the source to produce mordant dyes. The pollution of chromate anions has brought detrimental health effects attributed to accumulation in animal and human tissues [5]. Therefore, to prevent the anion from reaching the water systems, the search for materials that can separate this ion is crucial.

Recently, Density Functional Theory (DFT) has gained attention among researchers and is employed to conduct a comprehensive investigation into the properties of ligands. This approach could improve the understanding of anion-ligand complexes and facilitate the accurate determination of binding energies [6]. Significant geometric modifications were observed in the host through DFT optimization of the complexes, which were necessary to accommodate the binding of the anion. The DFT calculations indicate that the anion exhibits interactions with the NH groups and the aromatic protons. The finding of the previous study [7] is supported by their quantum chemical simulations, which demonstrated the significant involvement of NH and CH groups in phenyl protons in the binding of anions.

Along with this interest, in this study, two tetraamide compounds namely, 1,2-bis[*N,N'*-6-(4-pyridylmethylamido)pyridyl-2-carboxyamido]ethane (L1) and 1,2-bis[*N,N'*-6-(4-pyridylmethylamido)pyridyl-2-carboxyamido]propane (L2) have been utilized for anion study towards chromate. These compounds exhibit pre-organized amide structures and acidic functional groups of aminopyridine. According to a study, an aminopyridine functional group was added to the anion receptors molecule to acidify the CH and NH bonds, which made the receptor a better proton donor for hydrogen bonding [8].

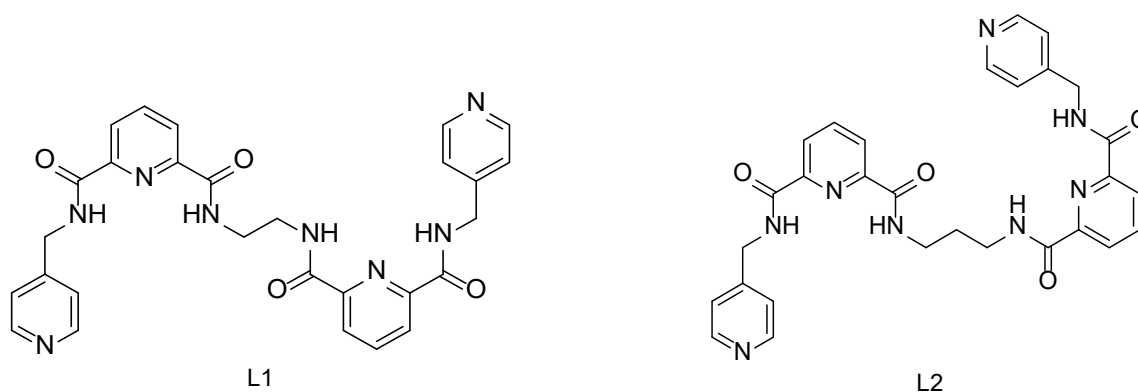


Figure 1 Structure of L1 and L2.

2.0 EXPERIMENTAL

2.1 Materials

Dimethyl-2,6-pyridinedicarboxylate, 4-aminomethylpyridine, dilute hydrochloric acid, sodium bicarbonate, sodium sulphate, ethane-1,2-diamine, propane-1,3-diamine, potassium chromate, methanol, toluene, dichloromethane, and acetonitrile were used in this study, without further purification. The synthetic methods are adapted and modified from the literature study [9].

2.2 Preparation of materials

The synthesis of these compounds (L1 and L2) involved *N*-6-[(4-pyridylmethylamino)carbonyl]-pyridine-2-carboxylic acid methyl ester (1.01 g, 3.7 mmol) with alkyl diamine in toluene (40 mL) and heated at reflux under an inert atmosphere, respectively. The alkyl diamine used for the L1 reaction was ethane-1,2-diamine (0.13 mL, 1.9 mmol), and the reaction duration was 55 hours; while for L2, the propane-1,3-diamine (0.15 mL, 1.8 mmol) was used, and the reaction occurred for 96 hours. Thin Layer Chromatography (TLC) was employed to monitor the reactions until completion. After the reflux process was completed, the solvent (toluene) was removed by using a rotary evaporator under reduced pressure (55°C at 70 mbar). Both reactions led to the formation of aqueous solutions, which underwent solidification for two days. These products for L1 and L2 were obtained as sticky yellow precipitates, with 1.07g (64%) and 0.89 g (52%) yields, respectively.

Synthesis of 1,2-bis[*N,N'*-6-(4-pyridylmethylamido)pyridyl-2-carboxyamido]ethane (L1)

Selected IR bands (FTIR, cm^{-1}): 3278 (m), N–H str. (asym); 2923 (m), C–H (str); 1666 (s), C=O str.; 1527 (s), N–H bend.; 1450 (s), C–H bend.; 1373 (s), C–N str.; 1072 (m), C=C.; 732 (s), C–H bend. ^1H NMR (400 MHz, $\text{DMSO-}d_6$); τ^m = 2.07 (2H, d, JHH = 6.8 Hz, H-1); 4.62 (2H, s, H-7); 7.32 (2H, d, JHH = 6 Hz, H-8); 8.22 (3H, m, H-3,H-4,H-5); 8.49 (2H, d, JHH = 6 Hz, H-9); 9.60 (2H, t, JHH = 6.4 Hz, H-2) and 9.96 (2H, t, JHH = 6.4 Hz, H-6). ^{13}C (100MHz, $\text{DMSO-}d_6$) ppm: δ = 21.09 (CH_2); 41.46 (pyCH_2NH); 121.98, 128.26, 128.95, 139.69, 148.28, 148.61, 149.67 (C-py); 163.24 and 163.72 (C=O). Anal. Calc. for $\text{C}_{28}\text{H}_{26}\text{N}_8\text{O}_4$ (538.56 g/mol): C, 62.44 %; H, 4.81 %; N, 20.81 %. Found: C, 62.03 %; H, 4.71 %; N, 20.01 %. Mp 263–265 °C.

Synthesis of 1,2-bis[*N,N'*-6-(4-pyridylmethylamido)pyridyl-2-carboxyamido]propane (L2)

Selected IR bands (FTIR, cm^{-1}): 3228 (m), N–H str. (asym); 2924 (m), C–H (str); 1658 (s), C=O str.; 1531 (s), N–H bend.; 1438 (s), C–H bend.; 1373 (s), C–N str.; 999 (s), C=C.; 736 (s), C–H bend. ^1H NMR (400 MHz, $\text{DMSO-}d_6$); τ^m = 1.73 (2H, q, H-1); 3.45 (2H, t, H-2); 4.63 (2H, d, JHH = 6.4 Hz, H-8); 7.31 (2H, d, JHH = 6 Hz, H-9); 8.24 (3H, m, H4,H5,H6); 8.49 (2H, d, JHH = 6.4 Hz, H10); 9.19 (1H, t, JHH = 6.4 Hz, H-3) and 9.32 (1H, t, JHH = 6.1 Hz, H-7). ^{13}C (100MHz, $\text{DMSO-}d_6$) ppm: δ = 29.91 (CH_2); 36.51 (CH_2); 41.48 (pyCH_2NH); 122.03, 124.50, 125.36, 139.67, 148.36, 148.92, 149.67 (C-py); 163.29 and 163.82 (C=O). Anal. Calc. for $\text{C}_{29}\text{H}_{28}\text{N}_8\text{O}_4$ (552.58 g/mol): C, 63.03 %; H, 5.11 %; N, 20.28 %. Found: C, 60.03 %; H, 5.44 %; N, 20.05 %. Mp 180–183 °C.

2.3 Characterization of materials

CHNS Analyzer Flash EA 1112 was used to record CHN elements. UV-Vis analysis was recorded using a Spectrophotometer Shimadzu UV-1800. Shimadzu ITRacer 100, Attenuated Total Reflection (ATR) was used for FTIR analysis (4000-400 cm^{-1}). ^1H and ^{13}C NMR were recorded using a Bruker Advance II 400 spectrometer.

2.4 Anion Titration Studies

2.4.2 UV-Vis Titration

Two stock solutions were freshly prepared in acetonitrile; one for compounds (10 mL, 3.33×10^{-5} M) and another for potassium chromate (10 mL, 2×10^{-5} M). In the titration experiment, a volume of 3 mL was transferred from the stock solution of chemicals into five volumetric flasks. Subsequently, the anions were added into individual volumetric flasks at varying volumes with 10 μL increments, starting from 10 μL to 50 μL .

3.0 RESULTS AND DISCUSSION

3.1 Characterization of L1 and L2

3.1.1 Infrared Spectroscopy

L1 and L2 have been successfully synthesized, showcasing significant alterations in the key functional groups of *N*-6-[(4-pyridylmethylamino)carbonyl]-pyridine-2-carboxylic acid methyl ester. Notably, the vibrational mode linked to the ester's C=O group (1735 cm^{-1}) has disappeared, while the vibrational mode of the amide's C=O group (1658 cm^{-1}) remains for both compounds. Moreover, conjugation in the molecule leads to chemical shifts in other functional groups. Figure 2 showed the FTIR spectra of L1 where several important peaks such as (C=O), (C-H)_{str}, (N-H)_{str}, (N-H)_{bend}, (C-H)_{bend}, (C=C) and (C-N)_{str} were indicated. FTIR spectrum shows (N-H) stretching of L1 and L2 in strong intensity at 3278 cm^{-1} and 3228 cm^{-1} , respectively. Other important peaks were observed at range $2923\text{-}2924 \text{ cm}^{-1}$, $1527\text{-}1531 \text{ cm}^{-1}$, $1438\text{-}1450 \text{ cm}^{-1}$, 1373 cm^{-1} , $1658\text{-}1666 \text{ cm}^{-1}$, and $999\text{-}1072 \text{ cm}^{-1}$ for (C-H)_{str}, (N-H)_{bend}, (C-H)_{bend}, (C-N)_{str}, (C=O) and (C=C), respectively. L2 has similar vibrational modes to those observed in L1. The FTIR data for L1 and L2 have been tabulated and shown in **Table 1**.

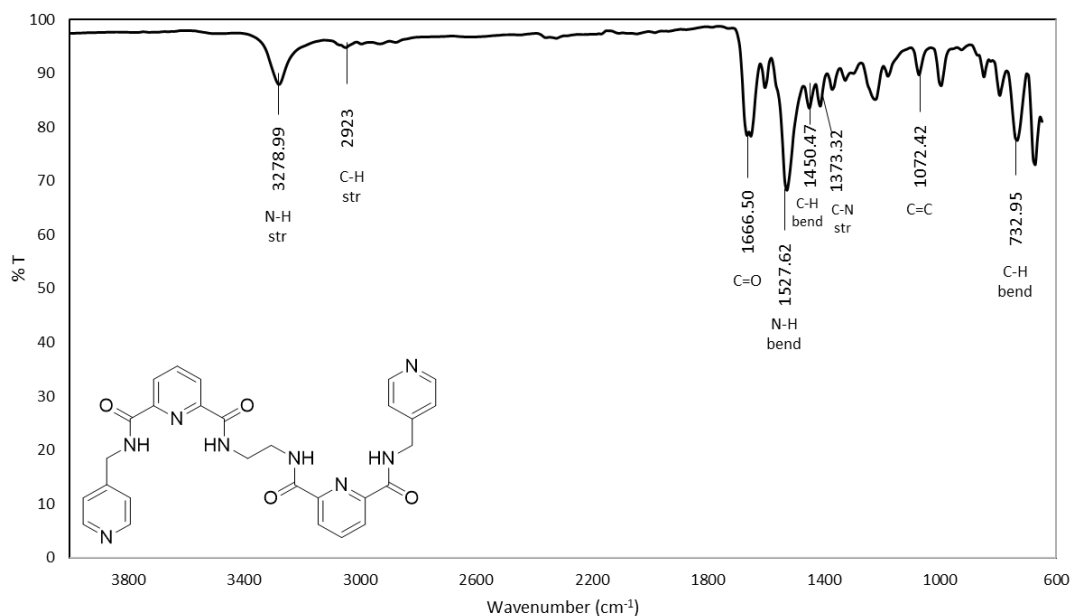


Figure 2 Infrared spectrum for L1.

Table 1 FTIR data for L1 and L2.

Vibrational Modes	Wavenumber (cm ⁻¹)		
	<i>N</i> -6-[(4-pyridylmethylamino)carbonyl]-pyridine-2-carboxylic acid methyl ester	L1	L2
N-H _{str}	3209	3278	3228
C-H _{str}	2954	2923	2924
C=O	1735	1666	1658
	1658		
N-H _{bend}	1535	1527	1531
C-H _{bend}	1435	1450	1438
C-N _{str}	1296	1373	1373
C=C	1002	1072	999
C-H _{bend}	732	732	736

3.1.2 ¹H and ¹³C NMR Spectroscopy

Figure 3 shows the ¹H NMR spectra of L1, which represents the common NMR trend for symmetrical species when two NH proton signals of NH amide were observed [10]. In the NMR spectrum of L1, the signals for ethyl protons were indicated at 2.07 and 4.62 ppm. Whilst signals for the protons at 2,6-pyridinediacarboxamide moieties appeared at 7.32, 8.22 and 8.49 ppm (Figure 3). The presence of two signature peaks representing NH amide (H-2) and NH pyridine (H-6) located in the downfield regions at 9.60 ppm and 9.94 ppm, respectively. NH is known as relatively electronegative; consequently, a deshielding effect occurs, resulting in an intensified magnetic field experienced by the protons. Furthermore, the downfield shift is effected by the neighbour carbonyl group (C=O), to the NH amide and N pyridine. Similar to L1, the proton peaks for propyl are indicated at upfield regions compared to L1. Compound L1 consists of an ethyl linker that is shorter compared to L2 that contains propyl, and this explains the appearance of (CH₂)_n at the downfield region. Jakob and colleagues [11] have also stated that the electronegativity of oxygen and nitrogen caused the downfield shift, as observed for L1. More signals of proton peaks of L2 were found at 4.63 ppm, aromatic pyridine of 2,6-pyridinediacarboxamide at 7.31 ppm, 8.24 ppm and 8.49 ppm. The NH signals were found at 9.19 ppm (NH linker) and 9.32 ppm (NH aminomethylpyridine). ¹H NMR data for L1 and L2 has been tabulated in Table 2.

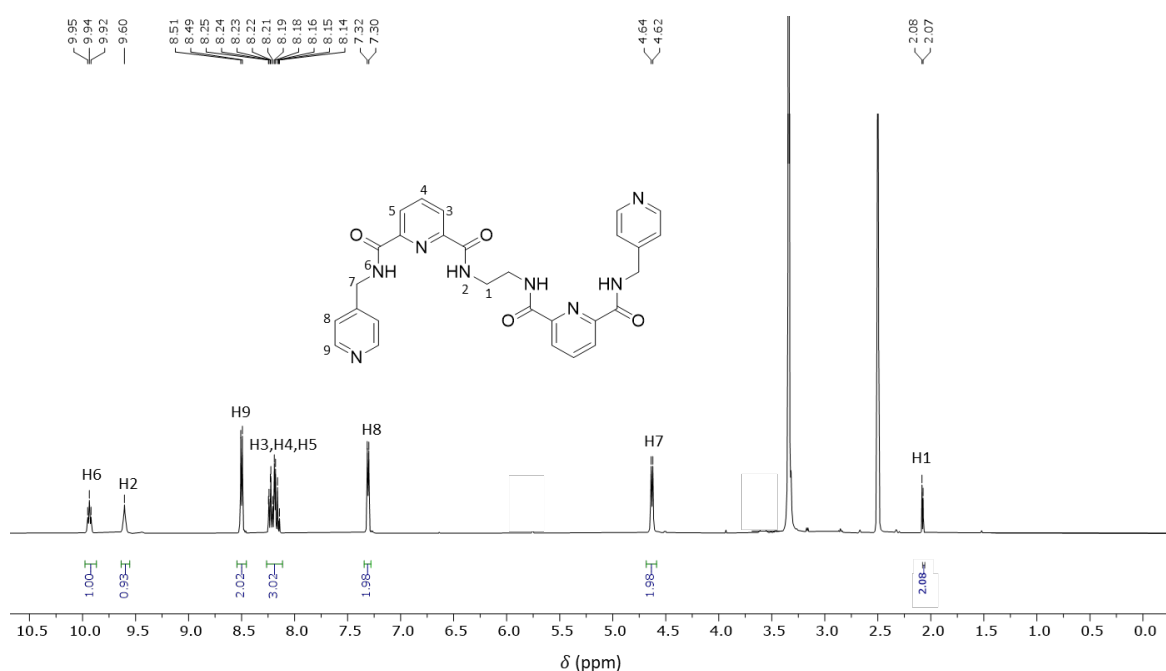
**Figure 3** ¹H NMR spectrum for L1

Table 2 ^1H NMR for L1 and L2.

Compound	Assignment	Moiety	Chemical shift (δ_{H} , ppm)
L1	H1	d, $J_{\text{HH}} = 6.8$ Hz, 2H, CH_2	2.07
	H7	d, 2H, pyCH_2NH	4.62
	H8	d, $J_{\text{HH}} = 6$ Hz, 2H, C_5H_4	7.32
	H3, H4, H5	m, 3H, C_5H_3	8.22
	H9	d, $J_{\text{HH}} = 6$ Hz, 2H, C_5H_4	8.49
	H2	t, 1H, CH_2NH	9.60
	H6	t, 1H, pyCH_2NH	9.94
L2	H1	q, 2H, $\text{CH}_2\text{CH}_2\text{NH}$	1.73
	H2	t, 2H, $\text{CH}_2\text{CH}_2\text{NH}$	3.45
	H8	d, 2H, pyCH_2NH	4.63
	H9	d, 2H, C_5H_4	7.31
	H4, H5, H6	m, 3H, C_5H_3	8.24
	H10	d, 2H, C_5H_4	8.49
	H3	t, 1H, $\text{CH}_2\text{CH}_2\text{NH}$	9.19
	H7	t, 1H, pyCH_2NH	9.32

^{13}C NMR signal for compound L1 is shown in Figure 4. The main difference that can be distinguished between the two compounds is the number of carbon signals of alkyls at the spacer. Ethyl spacer of L1 resulting was detected at 21.09 ppm, while the other carbon peaks were indicated at 41.46 ppm, 121.98 ppm, 128.26 ppm, 128.95 ppm, 139.69 ppm, 148.28 ppm, 148.61 ppm, 149.67 ppm, 163.24 ppm and 163.72 ppm. The $\text{C}=\text{O}$ of L1 was observed in the downfield region (163.24 ppm and 163.72 ppm) due to the shorter spacer present in L1, which was significantly affected by the electronegative atoms such as oxygen and nitrogen at the moieties. The carbon signals of L2 were found at 29.91 ppm, 36.51 ppm, 41.48 ppm, 122.03 ppm, 124.50 ppm, 125.36 ppm, 139.67 ppm, 148.36 ppm, 148.92 ppm, 149.67 ppm, 163.29 and 163.82 ppm. ^{13}C NMR for L1 and L2 has been tabulated in Table 3.

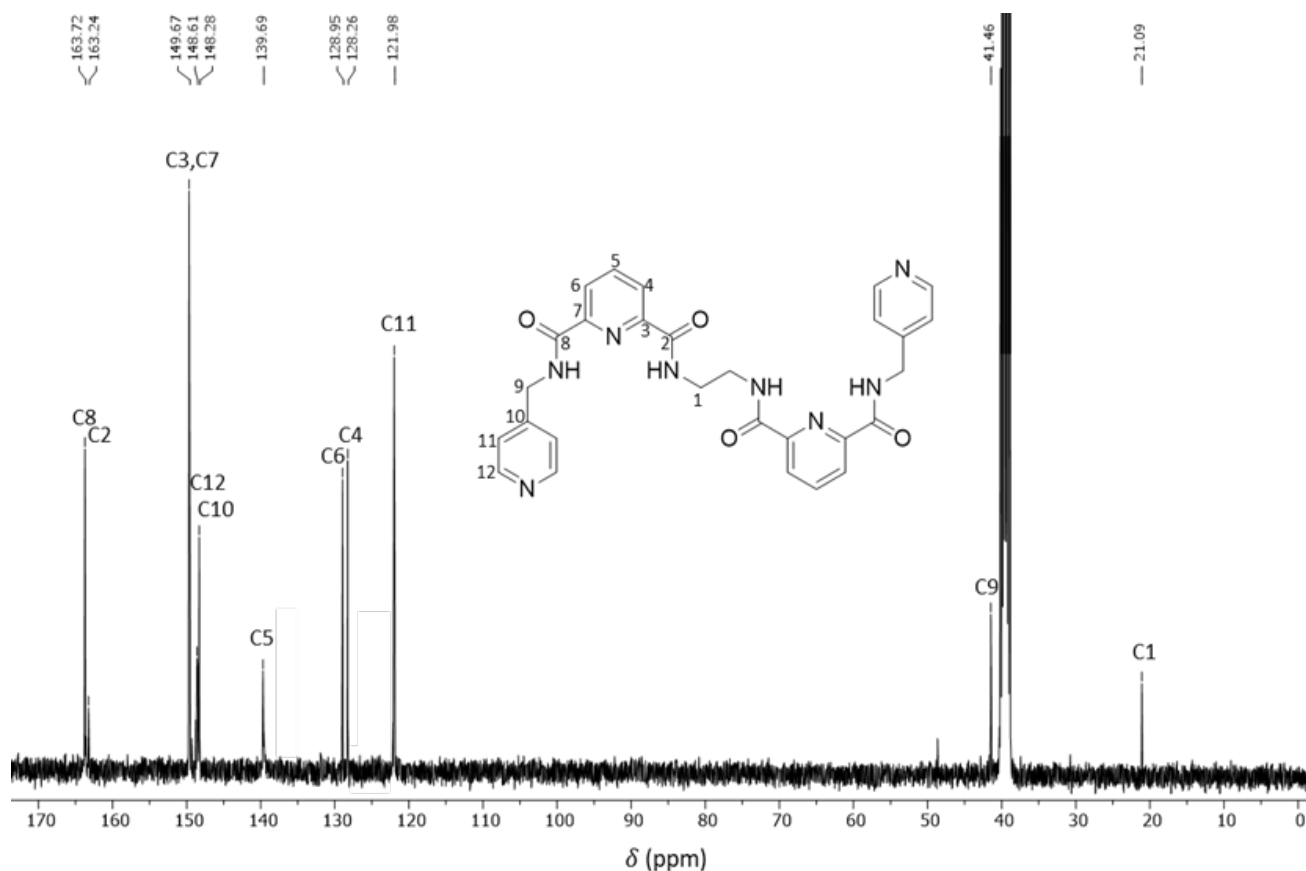
**Figure 4** ^{13}C NMR spectrum of L1

Table 3 ^{13}C NMR for L1 and L2.

Compound	Assignment	Moiety	Chemical shift(δ_{H} , ppm)
L1	C1	$\text{CH}_2\text{CH}_2\text{NH}$	21.09
	C9	pyCH_2NH	41.46
	C11	C=C	121.98
	C4	C=C	128.26
	C6	C=C	128.95
	C5	C=C	139.69
	C10	C=C	148.28
	C12	C=C	148.61
	C3, C7	C=C	149.67
	C2	C=O	163.24
C8	C=O	163.72	
L2	C1	$\text{CH}_2\text{CH}_2\text{NH}$	29.91
	C2	$\text{CH}_2\text{CH}_2\text{NH}$	36.51
	C10	pyCH_2NH	41.48
	C12	C=C	122.03
	C5	C=C	124.50
	C7	C=C	125.36
	C6	C=C	139.67
	C11	C=C	148.36
	C13	C=C	148.92
	C4, C8	C=C	149.67
	C3	C=O	163.29
C9	C=O	163.82	

3.1.4 DFT Studies

The calculations were conducted using the Gaussian 16 software and GaussView 5.0, performed by a high-performance computer (HPC) at Universiti Teknologi Malaysia (UTM). The geometries were fully optimized without any constraint on every bond length, bond angle, and dihedral angle. Geometry optimizations were conducted using the unrestricted DFT method at the level of B3LYP/6-311G (d,p). The basis set of 6-31G (d, p) is used for the C, H, N, and O atoms. According to the previous study, the *bis*-pyridyl-*bis*-amide ligand can afford varieties of conformations due to the flexible nature of the structure; therefore, the DFT study is used to determine the optimization energies for L1 and L2 in the form of either a U-shape (*cis*) or an S-shape (*trans*). From the calculation, it resulted that both L1 and L2 are stable in the form of S-Shaped (*trans* conformation) with lowest optimization energy -4783004.18 kJ/mol and -4886249.97 kJ/mol, respectively (Figure 5).

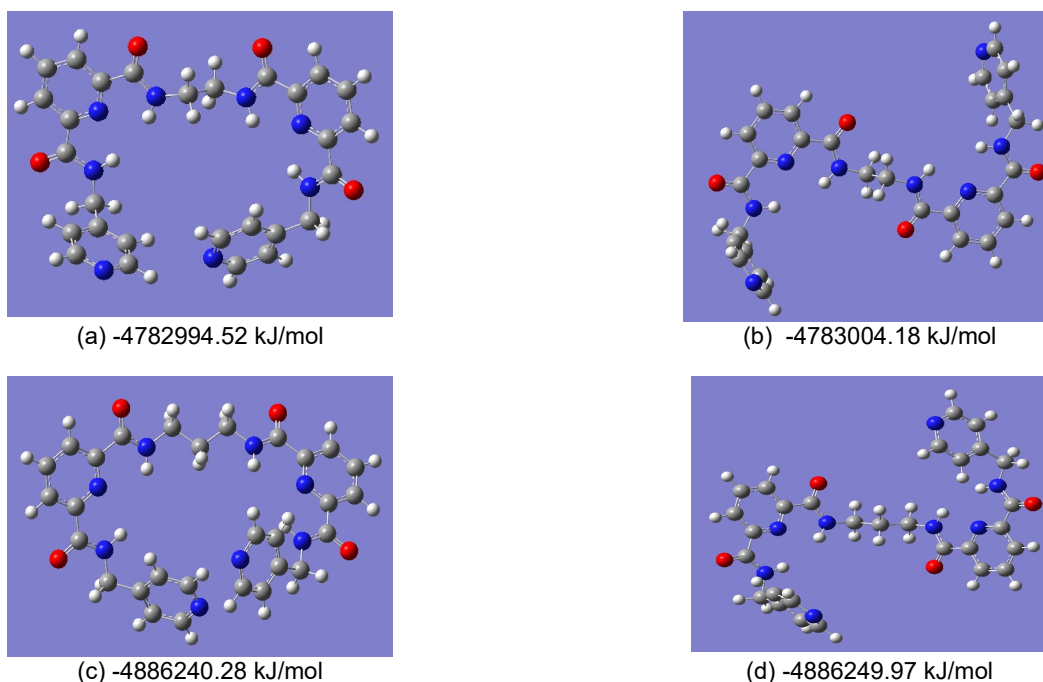


Figure 5 (a) L1 in *cis* form (b) L1 in *trans* form (c) L2 in *cis* form (d) L2 in *trans* form, with calculated optimization energies

3.2 Anion Titration Study

3.2.2 UV Vis Technique

UV titration towards potassium chromate was investigated. The titration result showed consistent changes in the interest peaks at 223 nm and 254 nm, respectively. After the consistent addition of potassium chromate, a constant change in absorbance was indicated, showing potential weak binding through hydrogen bonding interactions [12]. Figure 6(a) shows that when the concentration of chromate anion increased, the absorbance of dichromate anion at 353 nm also increased as expected. The evidence indicates that the solution contains a more significant number of anions that can interact with L1, which structurally has fewer steric factors compared to L2. An increased number of anions in a solution opened to an increased formation of the complex or the binding of the anions to L1 [13]. In return, the absorbance of the ligand at 223 nm gradually disappeared, indicating the presence of strong interaction or binding at the pyridine moieties as expected. In addition, the carbonyl peak absorbance at 254 nm underwent gradual redshifts to 266 nm along with the addition of dichromate anions. Titration of L2 with chromate anions also gave similar results but the absorbance changes were insignificant compared to L1 (Figure 6(b)). This result has shown that L1 has a good affinity towards chromate compared to L2. In a study conducted by López-Martínez et al. [14], a substantial decrease in the performance of complexes was seen with increasing alkyl chain length due to the steric effect. As the number of alkyl groups integrated into the molecule rises, the spatial volume approachable for forming the covalent bond with the electrophile decreases. Therefore, as the steric effect of a molecule increases, it may encounter obstruction in its capacity to undertake particular processes that facilitate conformational changes. The length of the spacer plays a crucial role in the flexibility of compounds, making them more challenging to control [15]. A longer alkyl chain also can reduce polarity and increase hydrophobicity compared to alkyl chains with shorter lengths which could lead to a higher degree of polarity.

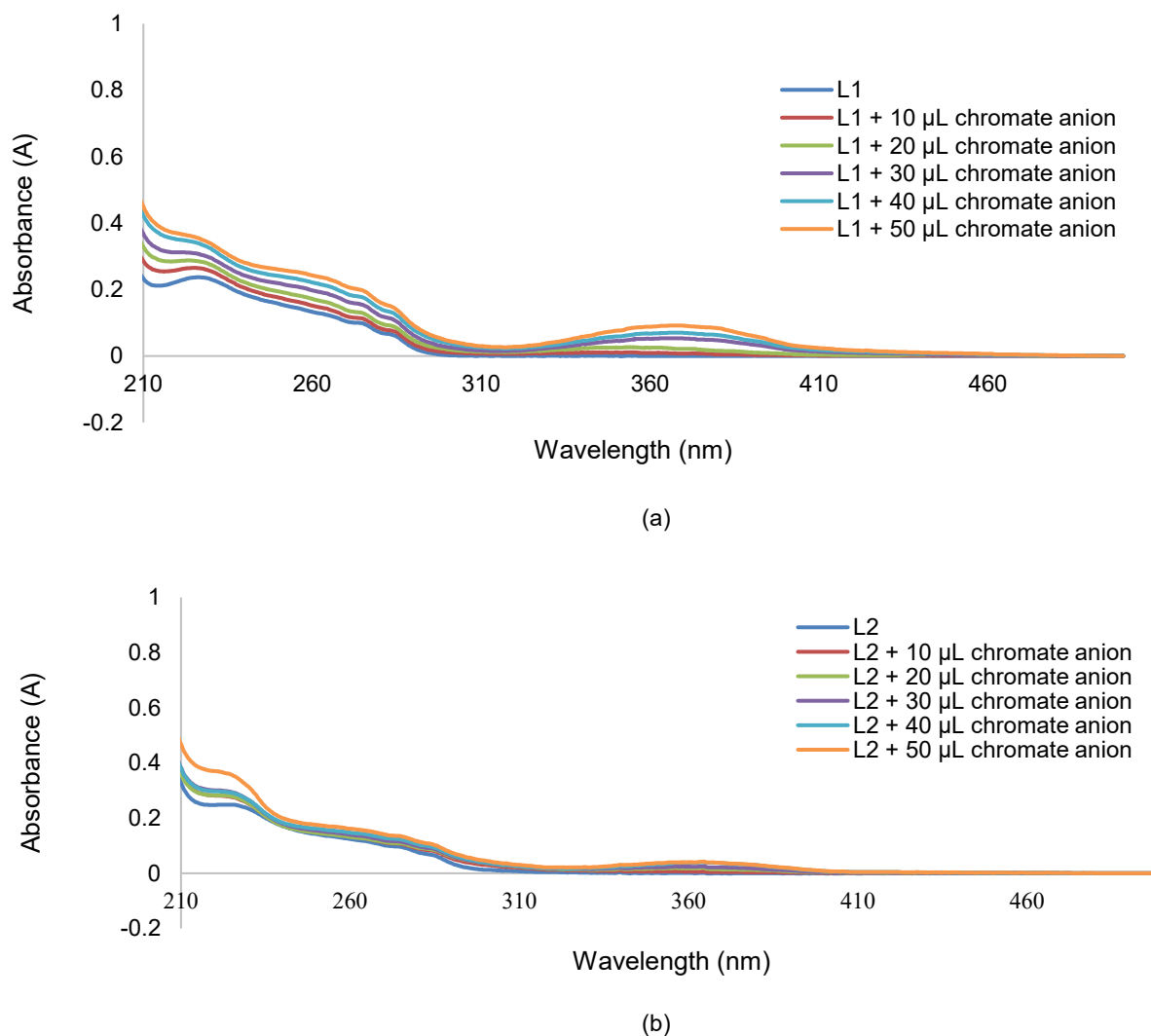


Figure 6 UV-Vis spectra for (a) L1 and (b) L2 when titrated with potassium chromate.

4.0 CONCLUSION

In summary, two pre-organized tetraamide compounds containing carboxamide NH binding hosts which are potentially designed as chromate receptors, L1 and L2 have been successfully synthesized and characterized by using spectroscopic methods. Investigation on the affinities of these two compounds towards chromate anions using UV-vis titration methods have been carried out and showed that L1 has a higher affinity towards chromate compared to L2. This supports many studies that proposed a smaller spacer unit in the molecular receptor, as this will contribute to a controllable binding to the host and less steric effects compared to lengthier spacers such as incorporated in L2.

Acknowledgement

This work was supported by FRGS (vot number 59579, FRGS/1/2019/STG01/UMT/02/3) from the Ministry of Higher Education, Malaysia and Universiti Malaysia Terengganu for scientific support.

References

- [1] Phuong, T., Cong, T. D., Ta, V. T., Nguyen, T. H. 2022. Study on Leaching of Phosphate from Municipal Wastewater Treatment Plant's Sewage Sludge and Followed by Adsorption on Mg-Al Layered Double Hydroxide. *Journal of Nanomaterials*. 2022: 1-9.
- [2] Cheng, X., Huang, X., Wang, X., Zhao, B., Chen, A., Sun, D. Sun. 2009. Phosphate Adsorption from Sewage Sludge Filtrate using Zinc-Aluminum Layered Double Hydroxides. *Journal of Hazardous Materials*. 169: 958–964.
- [3] Beniah, O. I., Christian, E. E., 2020. Pollution and Health Risks Assessment of Nitrate and Phosphate Concentrations in Water Bodies in South Eastern. *Nigeria, Environmental Advances*. 2020:1-8.
- [4] Bian, Z., Wang, Y., Zhang, X., Li, T., Grundy, S., Yang, Q., Cheng, R. 2020. A Review of Environment Effects on Nitrate Accumulation in Leafy Vegetables Grown in Controlled Environments, *Foods*, 9:732-740.
- [5] Bai, Y., Long, C., Hu, G., Zhou, D., Gao, X., Chen, Z., Wang, T., Yu, S., Han, Y., Yan, L. 2017. Association of Blood Chromium and Rare Earth Elements with The Risk of DNA Damage in Chromate Exposed Population. *Environmental Toxicology & Pharmacology*. 72: 103237.
- [6] Russ, T. H., Pramanik, A., Khansari, M. E., Wong, B. M., Hossain, M. A. 2012. A Quinoline Based bis-Urea Receptor for Anions: A Selective Receptor for Hydrogen Sulfate. *Natural Product Communications*, 7:301 – 304.
- [7] Navakhun, K., Techawan, V. 2019. Halide Recognitions of p-substituted Isophthamide-Based Anion Receptors: Experimental and Theoretical Studies. *Ramkhamhaeng International Journal of Science and Technology*, 3:23-29.
- [8] Martínez-Aguirre, M. A., Otero, D. M., Álvarez-Hernández, M. L., Torres-Blancas, T., Dorazco-González, Yatsimirsky, A. K. 2017. Anion and Sugar Recognition by 2,6-Pyridinedicarboxamide Bis-Boronic Acid Derivatives. *Heterocyclic Communications*. 23: 171-180.
- [9] Haris, N. S. H., Mansor, N., Yusof, M. S. M., Sumbly, C. J., Kadir, M. A. 2021. Investigating The Potential of Flexible and Pre-Organized Tetraamide Compounds to Encapsulate Anions in One-Dimensional Coordination Polymers: Synthesis, Spectroscopic Studies and Crystal Structures. *Crystals*. 11: 77-91.
- [10] Sumbly, C. J., Hanton, L. R. 2009. Syntheses and Studies of Flexible Amide Ligands: A Toolkit for Studying Metallo-Supramolecular Assemblies for Anion Binding. *Tetrahedron*. 65: 4681-4691.
- [11] Jakob, U, Petersen, T. O., Bannwarth, W. 2015. Unusual Metal complexes of *N,N*-bis(2-picoyl)amides - A Comparative Study of Structure and Reactivity. *Journal Organometallic Chemistry*. 797: 46-51.
- [12] Thordarson, P. 2011. Determining Association Constants from Titration Experiments Supramolecular Chemistry. *Chemical Society Review*. 40: 1305-1323.
- [13] Chen, L., Berry, S. N., Wu, X., Howe, E. N. W., Gale, P. A. 2020. Advances in Anion Receptor Chemistry. *Chem*. 6:61-141.
- [14] Lopez-Martinez, L.M., Garcia-Elias, J., Ochoa-Teran, A., Ortega, H.S., Ochoa-Lara, K., Montano-Medina, C.U., Yatsimirsky, A. K., Ramirez, J. Z., Labastida-Galvan, V., Ordonez, M. 2017. Synthesis, Characterization And Anion Recognition Studies Of New Fluorescent Alkyl bis(naphthylureylbenzamide)-based Receptors. *Tetrahedron*. 76:130815.
- [15] Roman, P., Julian, K., Kai, T., Louis F. B., Marvin, K., Andrea, M., Julia K., Suresh, K. V., Philip, A. C., Christian, S., Michael, T. W., Rasmus, L., Rochus, S., Sebastian, H. 2021. Frustrated Flexibility in Metal-organic Frameworks. *Nature Communications* .12:4097-4112.